Nuclear Instruments and Methods in Physics Research A 606 (2009) 790–794

Contents lists available at ScienceDirect

Nuclear Instruments and Methods in Physics Research A

journal homepage: www.elsevier.com/locate/nima

Shielding of the GERDA experiment against external gamma background

I. Barabanov [a], L. Bezrukov [a], E. Demidova [b], V. Gurentsov [a], S. Kianovsky [a], K.T. Knöpfle [c,*], V. Kornouhkov [a], B. Schwingenheuer [a], A. Vasenko [b]

[a] Institute for Nuclear Research, 60-letiya Oktyabrya prospekt 7a, Moscow 117312, Russia
[b] Institute for Theoretical and Experimental Physics, Moscow, Russia
[c] Max-Planck-Institut für Kernphysik, Saupfercheckweg 1, D-69117 Heidelberg, Germany

ARTICLE INFO

Article history:
Received 27 October 2008
Received in revised form
30 March 2009
Accepted 7 April 2009
Available online 18 April 2009

Keywords:
Double beta decay
Ge detector
Cryogenic liquid
Low background

ABSTRACT

The GERmanium Detector Array (GERDA) experiment will search for neutrinoless double beta decay of ^{76}Ge and is currently under construction at the INFN Laboratori Nazionali del Gran Sasso (LNGS) in Italy. The basic design of GERDA is the use of cryogenic liquid and water of high purity as a superior shield against the hitherto dominant background from external gamma radiation. In this paper we show by Monte Carlo simulations and analytical calculations how GERDA was designed to suppress this background at $Q_{\beta\beta}(^{76}\text{Ge}) = 2039$ keV to a level of about 10^{-4} cts/(keV kg y).

1. Introduction

Experimental investigations of solar, atmospheric, reactor and accelerator neutrinos have revealed the existence of neutrino oscillations providing clear evidence for non-zero neutrino masses. However, many properties of the neutrino need still to be determined. In particular, the very nature of the neutrino—Dirac or Majorana particle, the latter implying the neutrino to be its own anti-particle—is still unknown, and the study of neutrinoless double beta ($0\nu\beta\beta$) decay is the only practical experimental method for tackling this question. Moreover, the oscillation experiments have yielded the difference between the squares of the neutrino masses, and it is necessary to determine at least one absolute mass value or to obtain additional mass relations in order to establish the absolute neutrino mass scale. The region of interest below an effective neutrino mass $\langle m_\nu \rangle$ of 50 meV will not be reached by even the most advanced direct measurements [1,2]; it is, so far, accessible only by future $0\nu\beta\beta$ decay studies. From the measured half-life $T_{1/2}^{0\nu}$ of $0\nu\beta\beta$ decay the effective neutrino mass is deduced via the relation $\langle m_\nu \rangle^2 = m_e^2/(T_{1/2}^{0\nu} \times G^{0\nu} \times |M^{0\nu}|^2)$ where m_e is the electron mass, $G^{0\nu}$ a known kinematical factor and $|M^{0\nu}|$ the nuclear matrix element of the transition which has to be provided by a model calculation (see e.g. Refs. [3,4]).

Evidence for the $0\nu\beta\beta$ decay of ^{76}Ge has been recently claimed [5] on the basis of the data of the Heidelberg–Moscow experiment [6]. The result, if true, has fundamental consequences for particle theory, and requires further confirmation (see for discussion e.g. Ref. [7]). The sensitivity of a $0\nu\beta\beta$ experiment[1] scales with the product of source mass and exposure time, $M \cdot t$, as long as no background events are observed around the Q-value $Q_{\beta\beta}$ of the $0\nu\beta\beta$ decay; else the sensitivity scales only with the square root of this product divided by the background index (BI) and the energy window defining the signal region ΔE, $(M \cdot t/\text{BI}\,\Delta E)^{1/2}$ [4]. Thus a significant improvement of the experimental sensitivity is possible only by significant reduction of backgrounds. The background can be classified as 'external' originating from the experimental environment or 'intrinsic' due to contamination of the source and detector. The analysis of the background of the Heidelberg–Moscow experiment has shown it to be dominated by external gamma radiation, i.e. gamma rays emerging from the environment of the experiment and the cryostat materials [8]. In case of the IGEX experiment [9] the external and intrinsic background contributions were similar [10]. In both experiments [6,9], a background index of about 0.1 cts/keV kg y at the $Q_{\beta\beta}$ value of 2039 keV has been achieved. A reduction of the external gamma background from the cryostat and the environment can be achieved by either an increased passive shield made out of

[1] This quantity is defined by the lower half-live limit $T_{1/2}^{0\nu} \geqslant \ln 2N\varepsilon t/D$ where N is the number of source nuclei, ε the detection efficiency, t the exposure time and D the lower limit of the number of decays which can be excluded at a given confidence level.

* Corresponding author. Tel.: +49 6221 516509; fax: +49 6221 516603.
E-mail addresses: barabanovi@mail.ru (I. Barabanov), ktkno@mpi-hd.mpg.de (K.T. Knöpfle).

0168-9002/$ - see front matter © 2009 Elsevier B.V. All rights reserved.
doi:10.1016/j.nima.2009.04.006

materials of higher radiopurity and/or active shields. This paper discusses different design scenarios of the GERmanium Detector Array (GERDA) experiment which we studied in order to find a solution which is technically and economically feasible and which limits this previously important background contribution to a level of 10^{-4} cts/(keV kg y). The simulations show that our solution reaches this goal which is a prerequisite to reach a total BI of 10^{-3} cts/(keV kg y) in view of additional intrinsic background contributions and other sources of external background originating for example from detector holders, front end electronics and cables.

2. The GERDA experiment

The GERmanium Detector Array [11–13] is an experiment being constructed in Hall A of the Gran Sasso National Laboratory (LNGS), Italy. An array of bare germanium detectors, enriched in the isotope ^{76}Ge to a level of about 86%, will be suspended by a minimum of material inside a cryostat filled with a liquefied gas (see Fig. 1). It utilizes an earlier suggestion [14] to use ultrapure cryogenic liquids, nitrogen (LN_2) or argon (LAr),[2] both as cooling medium and as shield against the external gamma radiation. The cryostat is surrounded by an up to 3 m thick buffer of ultrapure water that acts as an additional gamma shield and suppresses neutron background to a negligible level [12]. Compared to an earlier proposal [15], this setup reduces the amount of cryogenic liquid to be stored underground significantly, and it is indeed rather similar to a further developed setup proposed in Ref. [16]. The muon induced background is identified and rejected to a level of BI $<10^{-4}$ cts/(keV kg y) by a water Cherenkov detector and plastic scintillators [17]. With this design, a total background index of about 10^{-3} cts/(keV kg y) at the $Q_{\beta\beta}$ value of2039 keV is envisioned if the intrinsic background is less than about 5×10^{-4} cts/(keV kg y), see Refs. [12,13] for more details. A phased approach is chosen for the experiment. In a first phase, eight detectors that were previously operated by the Heidelberg–Moscow and IGEX collaborations [6,9] will be redeployed. The detectors are of cylindrical shape ($h = 80$ mm, $\phi = 80$ mm) with a mass of about 2 kg, each. The main aim of the first phase is to scrutinize the previous claim [5] with an exposure of about 20 kg y. In a second phase, the sensitivity will be increased by using new Ge diodes made out of enriched ^{76}Ge material. This should allow to explore the region of an effective electron neutrino mass of about 100 meV. Here, we consider the requirements for shielding the Ge detectors against gamma radiation from the cryostat material and the concrete/rock of the laboratory such that the desired BI can be achieved.

3. The Monte Carlo simulations

The main contribution to the background at $Q_{\beta\beta} = 2039$ keV from external gamma radiation is due to the 2.6 MeV γ-line of ^{208}Tl which is produced in the decay chain of ^{232}Th. Other γ lines originating in the primordial U/Th decay chains with energies above 2 MeV exhibit significantly lower intensities; at equal activities of U and Th, ^{214}Bi contributes about 20% relative to ^{208}Tl at $Q_{\beta\beta}$. Thus all the calculations were done for the energy of this ^{208}Tl line. It is sufficient to simulate only this individual line and not the entire decay chain since the decays occur far from the detectors. We will consider first the contributions to the background from the radioactive admixtures in the cryostat material, which is crucial for the experiment, and then discuss the background from the gamma activity of the surrounding rock.

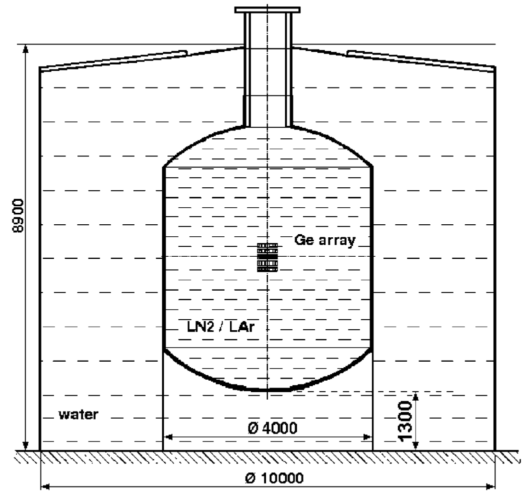

Fig. 1. Schematic of the GERDA cryostat for LN_2 or LAr, and the surrounding water tank. The height of water is 8.5 m. The location of the Ge detector array in the middle of the cryostat is indicated. Cryostat dimensions are shown in Fig. 3.

The best material for the cryostat is high purity copper which has been shown to exhibit a ^{228}Th activity of less than 20 μBq/kg [18]. Since a large volume copper cryostat implies, however, both safety and fabrication problems, we consider a cryostat built from stainless steel as well.

The Monte Carlo (MC) simulations have been performed using two approaches: (i) a dedicated simulation of the transport of gamma rays through the cryostat material and the cryogenic liquid to the detectors and (ii) an application of the standard program package GEANT4 [19] whose electromagnetic models have passed quantitative validation [20]. The results from both approaches are in agreement within their statistical accuracy of about 10% to 15% so that only one value is quoted in the following sections. Anti-coincidences between any two of the nine crystals were taken into account with an energy threshold of 10 keV in each crystal (see Section 4 for details on the geometry). The application of anti-coincidences lowers the BI value by about 30%.

For studying the effects of changes of the setup parameters on the BI, only the use of an analytical calculation instead of rather time-consuming MC simulations is realistic. By comparing the results of MC calculations with analytical ones it was found that identical results for the gamma background at $Q_{\beta\beta}$ can be obtained by using effective gamma absorption coefficients μ' that are by about 15% smaller than those (μ) for a narrow γ-beam: $\mu/\rho = 0.0380\,(0.0379)\,\mathrm{cm}^2/\mathrm{g}$ for LAr (LN_2) where ρ is the density of the respective liquid (1.394 (0.807) g/cm^3). This approach is different from the traditional ansatz using build-up factors to account for scattering effects in the shielding material [21,22]. Fig. 2 demonstrates the viability of the present approach by considering the attenuation of 2.615 MeV γ-rays in the center of a sphere of water as a function of the radius of the sphere. The MC results for the full energy peak are well reproduced with the known linear attenuation coefficient of $\mu \equiv K3 = 0.042\,\mathrm{cm}^{-1}$ at 2.615 MeV. As expected, for energy intervals below the full energy peak, the absorption is found less steep, and can be indeed fitted satisfactorily with exponential functions using the indicated exponents with respective errors of less than 3%.

4. Results and discussion

In the simulation, nine Ge crystals ($h = 80$ mm, $\phi = 80$ mm) are placed in the center of the cryostat. Two arrangements of the

[2] The long-lived argon isotopes ^{39}Ar and ^{42}Ar with half-lives of 269 y resp. 32.9 y do not generate background at $Q_{\beta\beta}$ being beta emitters with endpoint energies of 565 keV resp. 600 keV.

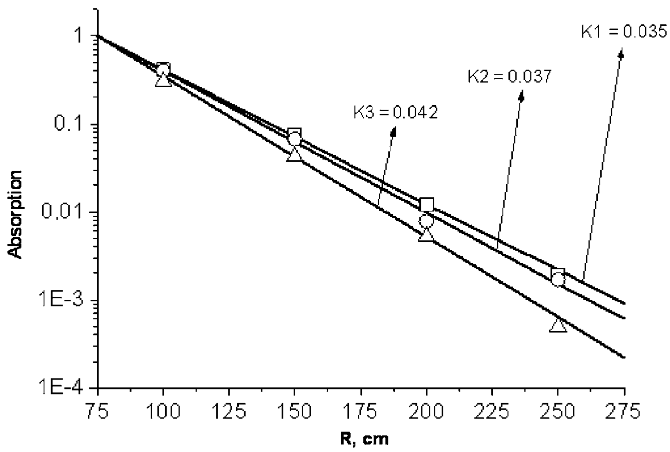

Fig. 2. Monte Carlo results for the attenuation of 2.615 MeV gamma rays in water. Plotted is the absorption (arbitrary scale) for a sphere of radius R for gamma quanta in the peak region 2600–2615 keV (triangles), as well as in the energy intervals 1800–2300 keV (circles) and 0–2615 keV (squares). The lines are exponential fits to the MC results with indicated linear attenuation coefficients $K1$, $K2$ and $K3$ in units of cm^{-1}; each coefficient has an error of 0.001 cm^{-1} at 90% confidence level.

crystals are considered: a plane 3×3 matrix, and three chains with three crystals in each chain (10 mm and 50 mm distance of closest approach horizontally and vertically, respectively). For both configurations, the calculated BI turned out to exhibit the same value within the statistical accuracy (10%) of our calculations, and only one value is presented in the following tables.

4.1. Background from the copper cryostat

A cross-section of the assumed copper cryostat is presented in Fig. 3. The inner diameter of the cryostat is 3.75 m, the total height 7.5 m and the total thickness of all copper walls is 5 cm. To warrant sufficient thermal insulation, the upper part of the cryostat's neck has to be fabricated from stainless steel. According to preliminary measurements, the ^{228}Th activity of the copper amounts to 25–10 μBq/kg, while that of stainless steel has been expected to be orders of magnitude higher, 10–1 mBq/kg. For the simulations, we assume the larger values.

The results of the simulation are presented in Table 1(a). It can be seen that a BI of a few 10^{-4} cts/(keV kg y) can be achieved with a copper cryostat and LN_2. With LAr filling the BI can be further reduced by a factor of 17.

4.2. Background from the stainless steel cryostat

The main parameters of the stainless steel cryostat (Fig. 3) are: an inner diameter of 4 m, a total height of 7.6 m and a total wall thickness of 3 cm. The results of the simulation for a ^{228}Th activity of 10 mBq/kg of the stainless steel are presented in Table 1(b). The background contributions from the cylindrical part and the upper and bottom vessel heads were calculated separately.

The BI for the stainless steel cryostat filled with LN_2 is found to be too high, and this setup will be no longer considered. Even filled with LAr the BI from the steel activity is still higher than required. To further suppress the background, a shield from a purer material (copper) on the inner surface of the cylindrical part of the cryostat is needed. To find the optimum profile, the contributions to the BI from different elements of the cylindrical shell have been determined as a function of their distance from the center of the cryostat ($z = 0$) by Monte Carlo simulations. The

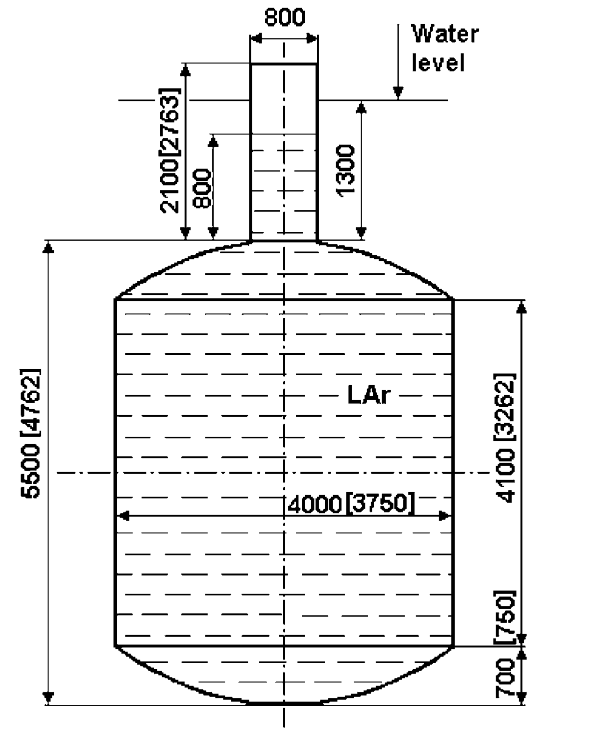

Fig. 3. Cross-sections of the copper and stainless steel cryostats. Dimensions for the copper cryostat are given in brackets units are mm.

Table 1
Calculated background index (BI) in 10^{-4} cts/(keV kg y) from the cryostat.

Device	BI [10^{-4} cts/(keV kg y)]	
(a) Copper cryostat	LN_2	LAr
Copper body	2.0	0.12
Steel neck	0.6	0.03
Total	2.6	0.15
(b) Stainless steel cryostat	LN_2	LAr
Cylindrical part	370	22 (1.1)
Top vessel head	15	0.26 (0.02)
Bottom vessel head	15	0.25 (0.12)
Total	400	22.5 (1.24)
(c) Stainless steel cryostat with internal shield of		
8.4 t Cu	–	12 ± 1
23 t Cu	–	2.8 ± 0.4
41 t Cu	–	0.72 ± 0.04

The setup consists of nine Ge crystals of 2 kg mass each in the center of a (a) copper, (b) stainless steel cryostat and (c) a stainless steel cryostat with indicated internal copper shield in its cylindrical part. The ^{228}Th activity of the copper and steel is assumed to be 25 μBq/kg and 10 mBq/kg, respectively. Values in parentheses denote the expected values for the GERDA steel cryostat as built with the measured activity.

results are shown in Fig. 4, top; for comparison the dependence for LN_2 is given as well. On the basis of these results, the optimum copper profile is found for background suppression factors of 30, 7.8 and 2, and presented in Fig. 4, bottom. The thickness of the additional shielding has been calculated analytically as described above, and after that, the BI for each profile was determined by MC simulations. The copper weights for these cases and the corresponding BIs are given in Table 1(c).

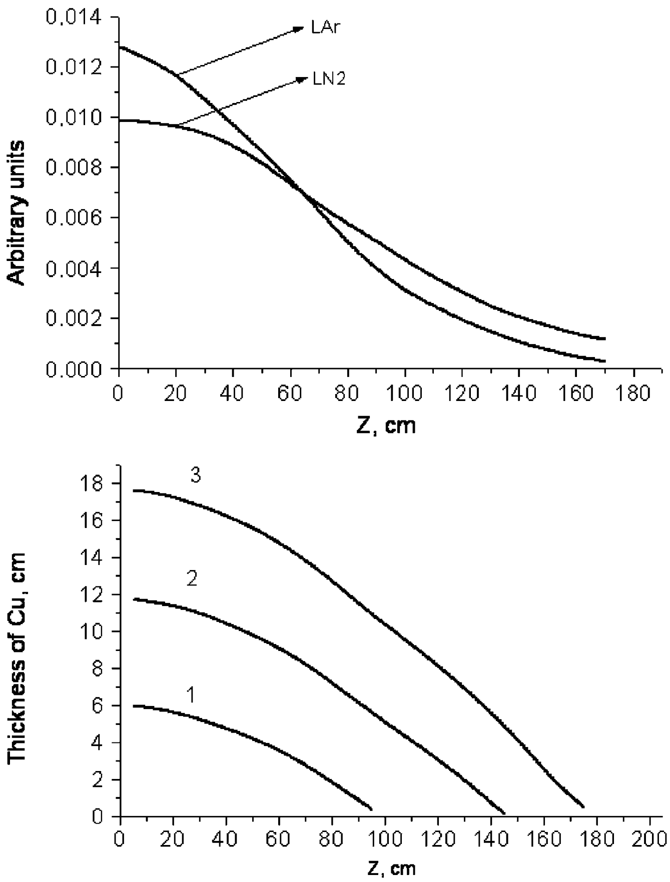

Fig. 4. (Top) Contributions of the cryostat's cylindrical parts to the background index as a function of the height $\pm z$ with $z = 0$ corresponding to the central plane. The curves for the LN_2 and LAr shielding media are normalized to 1. (Bottom) Deduced Cu profiles in case of LAr for background suppression factors of 30 (label 3), 7.8 (2) and 2 (1).

The above results show that a BI of $(1-3)\,10^{-4}$ cts/(keV kg y) can be achieved with a stainless steel cryostat and an inner copper shielding. The crucial point is the ^{228}Th activity in the stainless steel. In case of a ^{228}Th activity of less than 1 mBq/kg the copper shielding would be minimal, or not needed at all in the initial stages of the experiment. Actually, the stainless steel plates used for the construction of the GERDA cryostat exhibited average activities[3] from less than 1–4.5 mBq/kg [23]. The respective contributions are given in Table 1(b) in parentheses. Although the total sum is close to a BI of 10^{-4} cts/(keV kg y), an internal 3–6 cm thick copper shield has been installed to provide some safety margin, e.g. against 'hot spots'.

4.3. Background from the rock and concrete of Hall A

The flux of 2.6 MeV gamma rays from ^{208}Tl decays in the floor and the walls at the location of the GERDA experiment, Hall A of LNGS , has been measured with a Ge detector. It is approximately isotropic and amounts to 0.031 cts/(cm^2 s) [24]. The corresponding BI for a copper cryostat filled with LN_2 with a surrounding water shield in the geometry shown in Fig. 1 has been determined with MC calculations assuming the thickness of the stainless steel walls of the water tank to be 10 mm. The results listed in Table 2 identify the contributions originating from gamma rays which are incident from the side or from top and bottom. The variation of the various contributions reflects the different thicknesses of the water shield which is largest laterally. Special attention has to be paid to the background from gamma rays penetrating through the 'open' neck of the cryostat which is not shielded by water. Closing the hole in the neck with a 15 cm thick plate of lead reduces the BI by a factor of 55 yielding in this configuration a BI of a few 10^{-4} cts/(keV kg y).

Table 2
Calculated contributions to the background index (BI) in 10^{-4} cts/(keV kg y) due to the ^{228}Th radioactivity of the surrounding concrete and rock for nine Ge crystals of 2 kg mass each in the setup shown in Fig. 1 using the copper cryostat filled with LN_2 or the stainless steel cryostat with internal copper shield filled with LAr.

Geometrical origin	BI [10^{-4} cts/(keV kg y)]	
	Cu cryostat, LN_2	Steel cryostat w. Cu shield, LAr
Cylindrical part	1.1	0.004
Top	1.2	0.019
Neck	240	0.023
Neck with 15 cm Pb	0.24	
Bottom	1.9	0.031
Total (no Pb in neck)	244	0.077
Total with 15 cm Pb	4.4	

The statistical errors of the values quoted for the copper and steel cryostat are about 15% and 40%, respectively.

In case of LAr filling, the BI is lower by about a factor of 17 as mentioned earlier. With an activity of less than 3×10^{-5} cts/(keV kg y), it will be negligible. An even lower activity results for the stainless steel cryostat with LAr filling, see last column of Table 2. Compared to the copper cryostat, the height of the LAr column above the cryostat's center has been increased by more than 1 m. There is thus no longer the need for a lead shield in the neck which would have required additional mechanics for the insertion of the Ge detector array.

4.4. Estimate of external background for actual GERDA setup

The results of the case studies discussed above have been used to optimize the dimensions of water tank and cryostat of the GERDA experiment whose construction is close to be complete. The dimensions of the installed water tank are the same as shown in Fig. 1. The thickness of the stainless steel wall, however, is less than the 10 mm assumed in the simulations; it ranges from 8 mm at the bottom to 6 mm at top. Safety and cost issues prevented the construction of the originally planned copper cryostat. The actually built backup solution, a stainless steel cryostat for LAr with internal copper shield, has very similar dimensions as shown in Fig. 3: its inner diameter is 4.0 m, and the height of the major cryogenic volume is 5.55 m; the height of the neck has been slightly increased so that the LAr level in the neck is now 0.95 m instead of 0.8 m. The internal copper shield of a total weight of 16 tons exhibits a thickness of 3–6 cm.

Taking the background estimates for the stainless steel cryostat from Tables 1 and 2, the gamma background contributions from cryostat and surrounding rock incl. concrete amount to 1.24×10^{-4} and 0.077×10^{-4} cts/(keV kg y), respectively. Due to the internal copper shield the former number decreases by more than 50%. Hence the estimate for the total contribution of the external gamma background is about 0.5×10^{-4} cts/(keV kg y). Acknowledging statistical uncertainties of about 20% and systematic errors of similar order of magnitude it is gratifying to note

[3] For ^{226}Ra from the ^{238}U decay chain upper limits of the measured activities are at most a factor of 2 worse than for ^{228}Th and positive values are similar. Hence the initially made statement that the background is dominated by the 2.615 MeV ^{208}Tl line is correct.

that above number is conservative in the sense that it has been obtained with simulations using a less favorable geometry than realized in the GERDA setup.

5. Conclusion

The GERDA experiment will study neutrinoless double beta decay of ^{76}Ge with a sensitivity for its half-life that is about one order of magnitude better than that achieved in the previous experiments. The contributions to the background index from external gamma background from the cryostat and the surrounding laboratory have been quantitatively determined. Several scenarios were considered for the reduction of these backgrounds using copper or stainless steel cryostats with LN_2 or LAr filling which are immersed in a water tank. It is shown that a background index from these sources of less than 10^{-4} cts/(keV kg y) can be obtained for suitable choices of dimensions, radiopurity of building materials and cryogenic liquid. Based on this study and other constraints, a stainless steel cryostat with an internal copper shield and LAr as cryogenic medium has been built for GERDA with a layout that is very similar to that shown here. Further reductions of the background index might be achieved by using segmented detectors exploiting anti-coincidences between detector segments [25], and/or by using LAr as an active shield exploiting its scintillation light for the implementation of a veto signal.

Acknowledgments

This work was supported by Grants from INTAS 05-1000008-7996, SS-5573.2006.2 and RFFI 06-02-16674.

References

[1] J. Bonn, B. Bornschein, L. Bornschein, L. Fickinger, B. Flatt, O. Kazachenko, A. Kovalik, Ch. Kraus, E.W. Otten, J.P. Schall, H. Ulrich, Ch. Weinheimer, Nucl. Phys. B (Proc. Suppl.) 91 (2001) 273.
[2] KATRIN Collaboration, [arXiv:hep-ex/0109033], 2001.
[3] F. Simkovic, A. Faessler, P. Vogel, Phys. Rev. C79 (2009) 015502, and refs. therein.
[4] F.T. Avignone III, S.R. Elliott, J. Engel, Rev. Mod. Phys. 80 (2008) 481.
[5] H.V. Klapdor-Kleingrothaus, I.V. Krishoveina, A. Dietz, O. Chkvorets, Phys. Lett. B 586 (2004) 198;
H.V. Klapdor-Kleingrothaus, I.V. Krishoveina, Mod. Phys. Lett. A 21 (2006) 1547.
[6] M. Günther, J. Hellmig, G. Heusser, M. Hirsch, H.V. Klapdor-Kleingrothaus, B. Maier, H. Päs, F. Petry, Y. Ramachers, H. Strecker, M. Völlinger, A. Balysh, S.T. Belyaev, A. Demehin, A. Gurov, I. Kondratenko, D. Kotel'nikov, V.I. Lebedev, A. Müller, Phys. Rev. D 55 (1997) 54.
[7] A. Strumia, F. Vissani, [arXiv:hep-ph/0606054], 2007.
[8] Ch. Dörr, H.V. Klapdor-Kleingrothaus, Nucl. Instr. and Meth. A 513 (2003) 596 (and refs therein);
A.M. Bakalyarov, A.Ya. Balysh, S.T. Belyaev, V.I. Lebedev, S.V. Zhukov, Phys. Part. Nucl. Lett. 2 (2005) 77 [arXiv:hep-ex/0309016v1].
[9] D. González, J. Morales, S. Cebrián, E. García, I.G. Irastorza, A. Morales, A. Ortiz de Solórzano, J. Puimedón, M.L. Sarsa, J.A. Villar, C.E. Aalseth, F.T. Avignone III, R.L. Brodzinski, W.K. Hensley, H.S. Miley, J.H. Reeves, I.V. Kirpichnikov, A.A. Vasenko, A.A. Klimenko, S.B. Osetrov, A.A. Smolnikov, S.I. Vasiliev, V.S. Pogosov, A.G. Tamanvyan, Nucl. Instr. and Meth. A 515 (2003) 634.
[10] F.T. Avignone III, Private communication, 2008.
[11] The GERDA Collaboration, Letter of intent, [hep-ex/0404039], 2004.
[12] The GERDA Collaboration, Proposal ⟨http://www.mpi-hd.mpg.de/gerda/proposal_21sept.pdf⟩, 2004.
[13] S. Schönert, I. Abt, M. Altmann, A.M. Bakalyarov, I. Barabanov, C. Bauer, M. Bauer, E. Bellotti, S. Belogurov, S.T. Belyaev, A. Bettini, L. Bezrukov, V. Brudanin, C. Büttner, V.P. Bolotsky, A. Caldwell, C. Cattadori, M.V. Chirchenko, O. Chkvorets, H. Clement, E. Demidova, A. Di Vacri, J. Eberth, V. Egorov, E. Farnea, A. Gangapshev, G.Y. Grigoriev, V. Gurentsov, K. Gusev, W. Hampel, G. Heusser, W. Hofmann, L.V. Inzhechik, J. Jochum, M. Junker, S. Katulina, J. Kiko, I.V. Kirpichnikov, A. Klimenko, K.T. Knöpfle, O. Kochetov, V.N. Kornoukhov, R. Kotthaus, V. Kusminov, M. Laubenstein, V.I. Lebedev, X. Liu, H.-G. Moser, I. Nemchenok, L. Pandola, P. Peiffer, R.H. Richter, K. Rottler, C. Rossi Alvarez, V. Sandukovsky, S. Schönert, S. Scholl, J. Schreiner, B. Schwingenheuer, H. Simgen, A. Smolnikov, A.V. Tikhomirov, C. Tomei, C.A. Ur, A.A. Vasenko, S. Vasiliev, D. Weißhaar, M. Wojcik, E. Yanovich, J. Yurkowski, S.V. Zhukov, G. Zuzel, the GERDA collaboration, Nucl. Phys. Proc. Suppl. 145 (2005) 242.
[14] G. Heusser, Ann. Rev. Nucl. Part. Sci. 45 (1995) 543.
[15] H.V. Klapdor-Kleingrothaus, L. Baudis, G. Heusser, B. Majorovits, H. Paes, MPI-Report MPI-H-V26-1999 [hep-ph/9910205]; L. Baudis, G. Heusser, B. Majorovits, Y. Ramachers, H. Strecker, H.V. Klapdor-Kleingrothaus, Nucl. Instr. and Meth. A 426 (1999) 425.
[16] Yu.G. Zdesenko, O.A. Ponkratenko, V.I. Tretyak, J. Phys. G 27 (2001) 2129 [nucl-ex/0106021].
[17] L. Pandola, M. Bauer, K. Kröninger, X. Liu, C. Tomei, S. Belogurov, D. Franco, A. Klimenko, M. Knapp, Nucl. Instr. and Meth. A 570 (2007) 149.
[18] G. Alimonti, C. Arpesella, H. Back, M. Balata, T. Beau, G. Bellini, J. Benziger, S. Bonetti, A. Brigatti, B. Caccianiga, L. Cadonati, F. Calaprice, G. Cecchet, M. Chen, A. DeBari, E. DeHaas, H. de Kerret, O. Donghi, M. Deutsch, et al., Borexino Collaboration, Astropart. Phys. 16 (2002) 205.
[19] S. Agostinelli, J. Allison, K. Amako, J. Apostolakis, H. Araujo, P. Arce, M. Asai, D. Axen, S. Banerjee, G. Barrand, F. Behner, L. Bellagamba, J. Boudreau, L. Broglia, A. Brunengo, H. Burkhardt, S. Chauvie, J. Chuma, R. Chytracek, G. Cooperman, et al., GEANT4 collaboration, Nucl. Instr. and qMeth. A 506 (2003) 250; GEANT4 Collaboration, IEEE Trans. Nucl. Sci. NS-53 (2006) 270.
[20] K. Amako, S. Guatelli, V. Ivanchenko, M. Maire, B. Mascialino, K. Murakami, L. Pandola, S. Parlati, M.G. Pia, M. Piergentili, T. Sasaki, L. Urban, Nucl. Phys. B 150 (2006) 44.
[21] G. White, Phys. Rev. 80 (1950) 154.
[22] U. Fano, J. Res. Natl. Bur. Stand. 51 (1953) 95.
[23] W. Maneschg, M. Laubenstein, D. Budjas, W. Hampel, G. Heusser, K.T. Knoepfle, B. Schwingenheuer, H. Simgen, Nucl. Instr. and Meth. A 593 (2008) 448.
[24] O. Chkvorets, Ph.D. Thesis, Heidelberg ⟨http://www.ub.uni-heidelberg.de/archiv/8572⟩, 2008.
[25] I. Abt, M. Altmann, A. Caldwell, K. Kröninger, X. Liu, B. Majorovits, L. Pandola, C. Tomei, Nucl. Instr. and Meth. A 570 (2007) 479.